3. The cathodic charging technique indicates that two distinct oxygen species, most probably chemisorbed oxygen and nickel oxide, are formed on the surface.

4. Chemisorbed oxygen is reduced with a current efficiency close to 100% and gives a distinct arrest structure. Oxygen coverages can be determined since the roles of nonelectrochemical dissolution and parallel hydrogen evolution can be separated out from the cathodic reduction reaction.

5. The current efficiency for reduction of nickel oxide is poor and oxide coverages cannot be determined directly.

6. Oxidation initially gives nickel oxide at the active sites with simultaneous formation of NiO_{ads}, over the rest of the surface, up to a monolayer coverage. Further oxidation converts the NiO_{ads} to nickel oxide.

Manuscript submitted June 3, 1976; revised manuscript received Aug. 4, 1976.

Any discussion of this paper will appear in a Discussion Section to be published in the June 1977 JOURNAL. All discussions for the June 1977 Discussion Section should be submitted by Feb. 1, 1977.

Publication costs of this article were assisted by the National Research Council of Canada.

REFERENCES

1. B. MacDougall and M. Cohen, *This Journal*, **123**, 191 (1976).
2. B. MacDougall and M. Cohen, *ibid.*, **121**, 1152 (1974).
3. P. B. Sewell, B. MacDougall, D. F. Mitchell, and M. Cohen, Proceedings 6th International Congress on Metal Corrosion, Sydney, Australia (1975).
4. J. O'M Bockris, A.K.N. Reddy, and B. Rao, *This Journal*, **113**, 1113 (1966).
5. D. E. Davis and W. Barker, Proceedings 2nd International Congress on Metal Corrosion, New York, p. 551 (1963).
6. M. Okayama and S. Haruyama, *Corros. Sci.*, **14**, 1 (1974).
7. P. H. Holloway and J. B. Hudson, *Surf. Sci.*, **43**, 123 (1974); **43**, 141 (1974).
8. D. F. Mitchell, P. B. Sewell, and M. Cohen, *ibid.*, In press.
9. H. H. Uhlig, *Corros. Sci.*, **7**, 325 (1967).
10. C. R. Crowe and S. G. Fishman, *ibid.*, **13**, 569 (1973).
11. L. N. Yagupalskaya and B. A. Movchan, Proceedings 4th International Congress on Metal Corrosion, Amsterdam, p. 473 (1969).
12. R. M. Latanision and H. Opperhauser, *Corrosion (Houston)*, **27**, 509 (1971).
13. A. M. Laynon and B. M. W. Trapnell, *Proc. R. Soc. London, Ser. A*, **227**, 387 (1955).
14. N. Sato and M. Cohen, *This Journal*, **111**, 512 (1964).
15. H. A. Kozlowska, B. E. Conway, and W. B. A. Sharp, *J. Electroanal. Chem.*, **43**, 9 (1973).

Charge Transfer Processes during Anodic Polarization of Aluminum

K. Y. Kim,* R. D. Smith, and O. F. Devereux**

Institute of Materials Science and Department of Metallurgy, University of Connecticut, Storrs, Connecticut 06268

ABSTRACT

During prolonged anodizing of aluminum in aqueous 3 weight percent ammonium tartrate, ionic current components representing porous oxide development and aluminum dissolution were evaluated by gravimetry and optical absorbance, respectively, and compared to the total flow of charge measured in the external circuit. Electrolytes of *p*H 6.1 and 7 were studied. The dissolution of aluminum was markedly higher at *p*H 7, whereas the rate of porous oxide development was only slightly increased. In both cases an electronic current, obtained by difference, was evaluated, but it was very small at *p*H 7. At *p*H 7 a large nonelectrodic dissolution of aluminum was seen at the onset of anodizing. These observations are discussed in terms of steady-state processes in the barrier oxide layer involving both ionic transport and oxide dissolution.

Recent work has shown that a steady-state current develops during prolonged anodizing of aluminum in aqueous solutions of ammonium tartrate that is characteristic of the applied potential difference (1). It has been further shown that anodic films formed in this electrolyte, although traditionally regarded as "barrier-type," are, in fact, analogous to films formed in the traditionally "pore-forming" electrolytes (*e.g.*, sulfuric acid), both with respect to structure development and transient behavior of the anodic current at constant applied potential difference (2, 3). In attempting to understand both steady-state and transient aspects of the anodic current it is pertinent to know the nature of the charge transfer processes that occur at the anode. During development of a barrier oxide layer and, in pore-forming electrolytes, subsequent growth of a porous layer, the mode of charge transfer through the anodic oxide has been tacitly regarded as ionic for good and obvious reason. O'Sullivan and Wood, in their excellent treatise, discuss possible ionic processes in detail (4). The actual mechanism of ionic charge transfer is not certain, however, relatively recent tracer studies having supported cationic flow (5), anionic flow (6), and migration by both anions and cations (7, 8). While cationic current must be primarily due to aluminic ion, there may be a small protonic contribution (9, 10), and anionic current may be attributed to hydroxyl ions (9-12), oxide ions (8, 12), and acid anions (13, 14). In contrast, interest in anodic aluminum oxide films formed in "barrier-forming" electrolytes has stemmed largely from their ability to rectify alternating current. Again for obvious reason, the charge transfer mechanism in this case has been tacitly regarded as electronic, prompting considerable study of the role of both electronic and structural defects (11, 15-24). Electronic defects may arise either by hole injection at the metal/oxide interface, or electron injection at the oxide/electrolyte interface occasioned by oxygen liberation from water,

* Electrochemical Society Student Member.
** Electrochemical Society Active Member.
Key words: aluminum oxide, anodic oxidation, polarization, charge transfer.

hydroxyl ion, or other oxyanions. Diggle *et al.* (25) have suggested that the charge transfer mechanism in barrier-type films is field dependent; at high fields, the film is growing and both electronic and ionic flow occur, whereas at low fields this is not the case, only electronic flow being seen. Clearly the growth of a porous oxide layer on prolonged anodizing even in barrier-forming electrolytes, cited above (2, 3) and previously noted by others (26-28), is indicative of ionic flow under steady-state conditions.

The present study was performed to distinguish between ionic and electronic currents passed during prolonged anodizing of aluminum in a barrier-forming electrolyte. This was accomplished by measuring (*i*) the total current, and (*ii*) the ionic current, the latter being represented by the appearance of aluminum in the oxide film and also dissolved in the electrolyte. The electronic current (*iii*) was then established as the difference between (*i*) and (*ii*) above.

Experimental Procedures

Anodic oxide films were formed on cylindrical specimens, approximately 1 cm long and 1/2 cm in diameter, prepared from 1/4 in. diameter rod of 99.9995% or 99.999% purity (obtained from Materials Research Company and Leico Industries, Incorporated, respectively). The specimens were center drilled and tapped on one end for incorporation into a specimen assembly described by Greene (29), mechanically polished to 600 grit SiC paper, degreased with benzene followed by methanol, and finally rinsed with doubly distilled water. Some specimens were annealed at this stage of preparation for 1 hr at 80°C, but this was found to have no effect on the experimental results. Subsequently the specimens were chemically polished for 20 min in a solution of 3 parts nitric acid, 80 parts phosphoric acid, and 17 parts distilled water, rinsed with doubly distilled water, and dried with warm air.

Anodizing was conducted in a standard six hole Corning polarization cell, described by Greene (29). This incorporated two platinum counterelectrodes as well as the aluminum working electrode, a thermometer, and a gas inlet tube by which the electrolyte was continuously purged with nitrogen. Before each experiment all assemblies were meticulously cleaned with detergent, followed by concentrated hydrochloric acid, and thoroughly rinsed with doubly distilled water. All experiments were conducted at 30° ± 0.5°C. The anodizing electrolyte was a solution of 3 weight percent (w/o) reagent grade ammonium tartrate in doubly distilled water. In one portion of the work this solution was used as-prepared, having a *p*H value of 6.1; in other experiments it was titrated with dilute ammonium hydroxide to *p*H 7. The cases have been distinguished in reporting the results. In all experiments the anodic current was initially controlled at 1 mA/cm^2 until the anodizing potential reached 50V. This required approximately 5 min. Subsequent to this point in each experiment the potential was controlled at 50V. Experiments were terminated after intervals ranging from the point at which constant potential was imposed to 64 hr.

Several experiments were run for each anodizing time; except as noted all results are reported as averages determined from actual experimental values, with the data spread indicated where possible. For each experiment the following measurements were made:

(*a*) Total charge passed. Total charge passed after a given anodizing time was determined by integrating the as-recorded anodic current over time, using Simpson's rule. Values were normalized by division by individual, as-measured specimen areas.

(*b*) Oxide film weight. Two methods were used to determine the weight of oxide film formed during anodizing. In one technique the anodized specimens were carefully washed with doubly distilled water, then with methanol, and dried in a dessicator. The films were then removed by immersion of the specimens in a saturated aqueous mercuric chloride solution. The films were rinsed in doubly distilled water and again in methanol. The lower surface tension of methanol as compared to that of water reduced the degree of distortion seen in the films on drying. The dried films were weighed with a Cahn RG electrobalance; repetitive measurements showed a reproducibility of 1 μg. The films were not removed intact; in order to obtain the area represented by each weight measurement the films were photographed together with a scale and the areas of the resulting images were determined with a planimeter.

The other technique involved making three weight determinations for each specimen: (*i*) weight before anodizing, (*ii*) weight after anodizing, and (*iii*) weight after removal of the anodic film. Weight (*ii*) minus weight (*iii*) constituted the weight of the oxide film, while weight (*i*) minus weight (*iii*) represented the total aluminum reacted. Oxide film removal was accomplished by repeated brief immersions in a hot phosphoric-chromic acid solution (30), with degree of film removal being monitored by weight measurement.

The second of these methods provided an additional evaluation of the total amount of aluminum reacted, providing an internal check for each experiment, but was less sensitive than the first method due to the greater mass being weighed. Results using the two methods were in agreement.

(*c*) Aluminum dissolved in the electrolyte. Although this could be determined indirectly by the second gravimetric technique described above, it was measured directly for each experiment using an optical absorbance technique, ASTM Standard D857-69, Method C (31). This method was modified by omission of correction procedures for iron and fluoride, and by preparing standard solutions for calibration with fresh anodizing solution rather than with distilled water. A Cary spectrophotometer Model 14R was used.

In addition to the measurements described above selected films and substrates were examined using a Phillips EM300 transmission electron microscope and a Cambridge scanning electron microscope, respectively.

Results

Typical anodic current *vs.* time curves are shown in Fig. 1 for *p*H 6.1 and 7. The behavior of anodizing current over extended periods of time is analogous to that previously reported (1, 2). A dependence of current on *p*H is evidenced, with current values being higher for *p*H 7 than for *p*H 6.1. The total charge passed is shown as a function of time in Fig. 2. Since the anodizing current is virtually constant after the first few hours, the charge passed is linear with time, with a nonzero intercept indicative of the relatively high current passed during the initial constant current region of anodizing. The slopes for *p*H 6.1 and 7 are 21.44 and 28.14 μA/cm^2, respectively. The oxide film weight, shown *vs.* anodizing time in Fig. 3, exhibits a

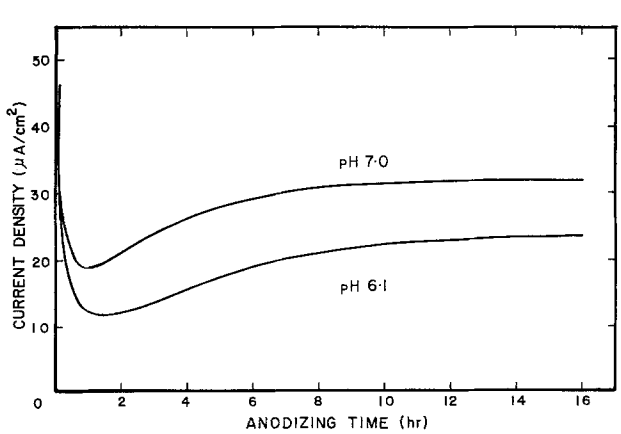

Fig. 1. Anodizing current *vs.* time

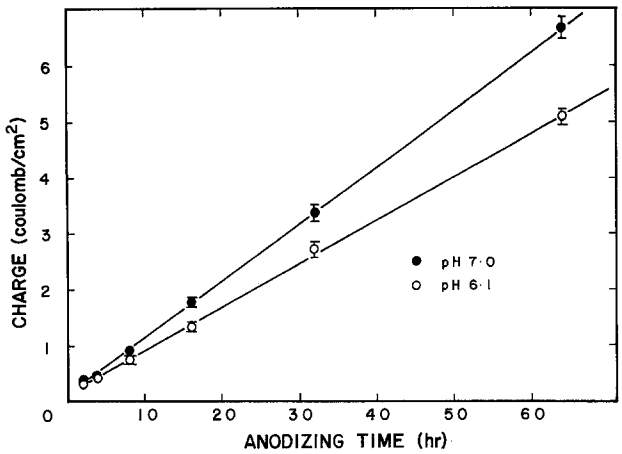

Fig. 2. Total charge passed per unit area vs. time

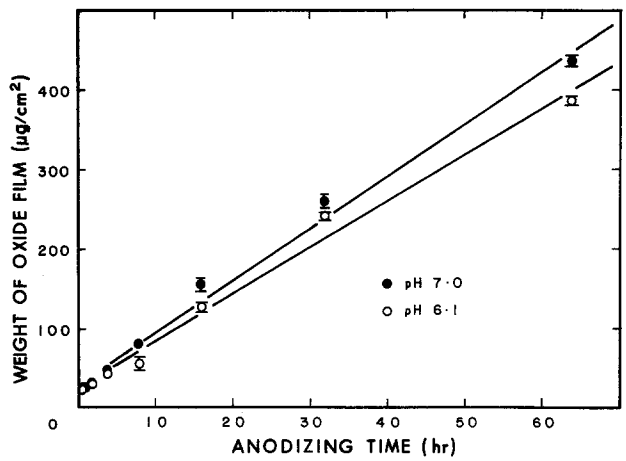

Fig. 3. Weight of anodic oxide per unit area vs. time

similar behavior, being approximately linear[1] with slopes of 5.84 and 6.57 μg/cm^{2}hr at pH 6.1 and 7, respectively. Again, a nonzero intercept is seen, representative of rapid film formation under constant anodic current. The amount of aluminum dissolved in the anodizing electrolyte is shown in Fig. 4. Again, the behavior is approximately linear,[1] with a substantial dependence on pH, the slopes being 2.84 and 5.75 μg/cm^{2}hr for pH 6.1 and 7, respectively. A near zero intercept and small experimental scatter are seen at pH 6.1, while at pH 7 the intercept is approximately 90 μg/cm^2 and the scatter in analyses is substantial.

Transmission electron microscopy revealed pore development similar to that previously described (2), with pore initiation approximately coincident with the minimum in anodizing current shown in Fig. 1. With the use of stereo pairs (2), it was possible to directly measure the barrier layer thickness to be 625 $\pm$ 15Å, corresponding to an anodizing constant of 12.5 $\pm$ 0.3 Å/V. SEM examination of the substrates revealed a substantial surface roughness, characteristic of chemical polishing.

[1] Were the error brackets extended to the 95% confidence limits on the mean of each data set, the relationship would be linear. For convenience in the ensuing discussion, linearity is assumed.

Discussion

As noted in the preceding, a basic premise of this study was that the ionic current passed through the oxide could be accounted for by the appearance of aluminum as oxide and as aluminate ion dissolved in the electrolyte. It was further presumed that the difference between this value and the total current passed must represent electronic current. To facilitate comparison data from Fig. 3 and 4 were converted to equivalent charge, assuming that the oxide was stoichiometric Al_2O_3 and that three equivalents of charge were passed for every gram atomic weight of aluminum oxidized. Figures 5 and 6 depict these comparisons for pH 6.1 and 7, respectively. The comparison for pH 6.1 is straightforward; the sum of the two ionic components of the charge passed, subtracted from the total charge passed, yields a net charge flow which must be attributable to electronic flow. This is not true at pH 7, where the sum of the ionic components is more than can be accounted for by the observed flow of charge through the external circuit.

This apparent discrepancy may be explained as follows. At pH 6.1 the charge representing dissolved aluminum has a zero intercept, indicating that the rate of dissolution essentially is constant in time. The total charge and the charge representing the oxide film have essentially identical positive intercepts, representing the initial high current period of anodizing. At pH 7, on the other hand, the charge flow due to dissolved aluminum, although linear, has a large positive intercept, representing a high dissolution rate at the onset of anodizing. This high rate is effective only for a brief period (results not shown in Fig. 6 suggest a period of less than 30 min of anodizing), beyond which the dissolution rate diminishes to a relatively small, constant value. The initial rapid dissolution of aluminum is clearly a nonelectrodic process, inasmuch as there is insufficient charge flow in the external circuit to account for the oxidation of all of the aluminum by electrodic processes. (As an example of such a nonelectrodic process, we suggest reduction of one or both

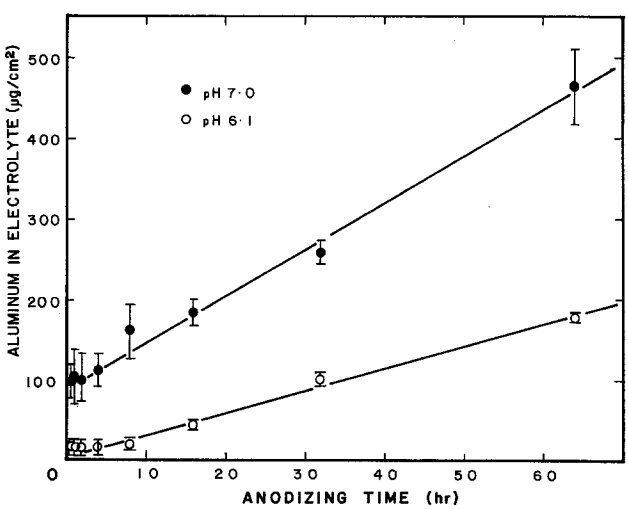

Fig. 4. Weight of aluminum in electrolyte per unit area vs. time

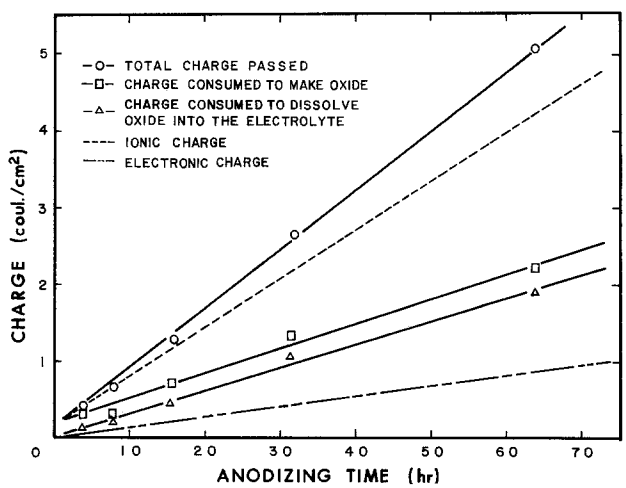

Fig. 5. Ionic and electronic contributions to total charge flow, pH 6.1.

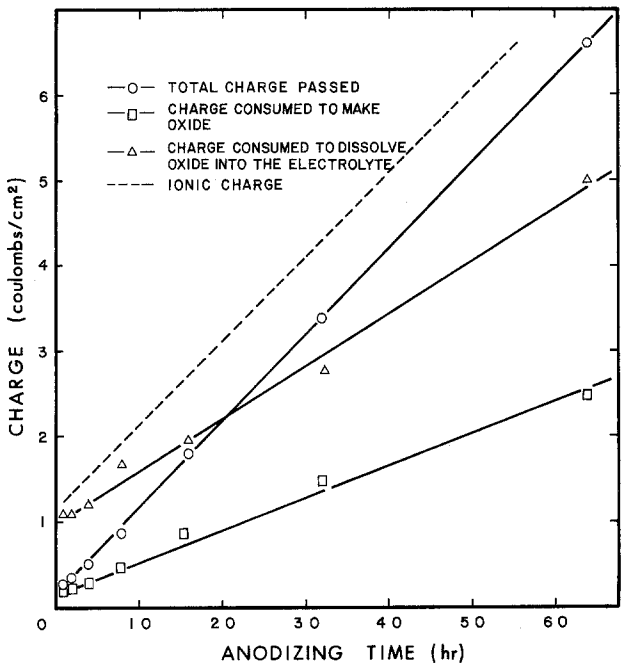

Fig. 6. Ionic contributions to total charge flow, pH 7

carboxyl groups on the tartrate ion by aluminum as more likely than evolution of hydrogen from hydroxyl ion or water due to the overwhelming tartrate concentration and the weaker nature of the carbon-oxygen bond as compared to the hydrogen-oxygen bond. These postulated reactions may be written, respectively

$$3C_4H_4O_6^{=} + 4Al + 3H_2O \rightarrow (C_4H_6O_5^{=})_3Al^{3+} + 3AlO_2^{-} \quad [1]$$

$$3C_4H_4O_6^{=} + 8Al + 6H_2O \rightarrow (C_4H_8O_4^{=})_3(Al^{3+})_2 + 6AlO_2^{-} \quad [2]$$

The reaction products are alcohols in which an ionic aluminum-oxygen bond has replaced a covalent hydrogen-oxygen bond.) Such a reaction will diminish markedly in rate as the anodic oxide develops; consequently, the nonelectrodic dissolution is expected to be least significant in environments in which the anodic oxide is least soluble and therefore, develops most rapidly. In this regard it may be shown that anhydrous α-Al_2O_3 exhibits minimum solubility in the vicinity of pH 5 (32). At higher pH, therefore, the solid oxide experiences a greater frequency of interaction with solvating hydroxyl ions via the reaction

$$Al_2O_3 + 2\,OH^- \rightarrow 2AlO_2^- + H_2O \quad [3]$$

so that the rate of dissolution as well as the equilibrium solubility must increase with increasing pH. Clearly, initial formation of the barrier oxide must progress more slowly at higher pH, allowing more time for nonelectrodic dissolution in agreement with observation. (Although we recognize that there is considerable variation in the solubility data pertaining to the various morphological forms of aluminum oxide, and that the anodic oxide may be more properly regarded as a pseudo-amorphous γ-Al_2O_3 rather than α-Al_2O_3 (33), we believe this argument to be qualitatively correct.)

Although the occurrence of a nonelectrodic process precludes meaningful comparison of the components of the total charge passed at pH 7, it is clearly a discrete event pertaining only to the onset of anodizing and does not preclude comparison of components of the steady-state current developed after several hours of anodizing. Such currents, *i.e.*, the slopes of the curves in Fig. 5 and 6, are listed in Table I. These values clearly indicate that the steady-state anodic current can be fully explained by electrodic reactions involving both ionic and electronic currents.

Table I. Steady-state anodic current components

pH	Net current	Al as oxide	Dissolved Al	Total ionic current	Electronic current*
6.1	21.44**	9.21	8.46	17.67	3.77
7	28.14	10.64	17.13	27.77	0.37

* By difference.
** Current reported in $\mu A/cm^2$.

In discussing the values reported in Table I it is instructive to make use of the oxide growth/field-assisted dissolution model for porous oxide development (4, 9) depicted in Fig. 7. In this model a stable barrier oxide layer is presumed to exist, representing a steady-state balance of oxide growth due to field-assisted ionic transport on the one hand, and field-assisted dissolution of the oxide by the electrolyte on the other. A portion of the oxide dissolved by the electrolyte is presumed to precipitate to form a growing porous structure whose presence does not significantly affect the steady-state processes in the barrier layer. Recent dielectric studies have shown that the resistance of the film is dominated by the barrier layer even in the presence of a porous oxide layer orders of magnitude thicker (34). Components pertaining to barrier oxide development are plotted *vs.* field strength in the barrier oxide. To a first approximation, the rate of transport of ions through the oxide can be regarded as exponential with respect to the field (15), while a linear dependence of oxide dissolution on field has been previously assumed and found to be valid in describing the increase of pore diameter and depth with time (2). It is useful, but not essential, to regard the field strength as inversely proportional to barrier layer thickness, although it is clear that this represents an oversimplification (35). No significant dependence of ionic transport on pH is expected; however, as discussed above it may be assumed that the oxide dissolution rate will be higher at pH 7 than at pH 6.1, as illustrated. The dashed curves in Fig. 7 represent the net growth rate of the barrier layer, with the terminal or steady-state barrier layer being represented by zero growth rate.

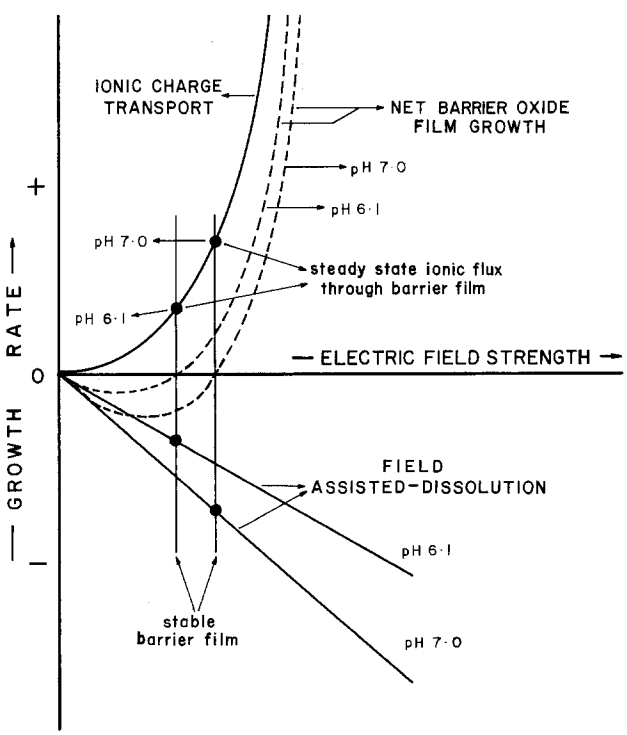

Fig. 7. Schematic representation of steady-state processes in the barrier layer.

The steady-state flux of ions through the oxide is clearly greater at pH 7 than at pH 6.1, reflecting the greater value of the field at steady state. This is in agreement with the values of total ionic flux reported in Table I. This model provides, however, no basis upon which to separate the total ionic flux into components representing growth of porous oxide and dissolution. Empirically, the growth rate is relatively insensitive to pH while, in agreement with the foregoing discussion, the dissolution rate is markedly enhanced by increase in pH in this range.

The observed dependence of electronic current on pH must be associated with a pH dependence of reducing agents at the oxide/electrolyte interface. Smith (22) has suggested electron injection by hydroxyl ions as the origin of the electronic current, although he and others later espoused a "weak spot" theory for conduction in anodic films (23, 15, 24). If electron injection by hydroxyl ion oxidation, in fact, occurs, the increased availability of hydroxyl ion at higher pH would suggest an increased electronic current. On the other hand, the data indicate a marked increase in the dissolution of oxide with increase in pH, effectively consuming near-surface hydroxyl ions by means of reaction (3). In other words, the higher flux of aluminum through the oxide/electrolyte interface may reduce the residence time of hydroxyl ions at the surface, thereby reducing the probability of an oxidation event. It is also possible to postulate oxidation of the tartrate hydroxyl groups as the electron injection mechanism, again with the increased instability of the surface oxide as the reason for reduced levels of injection at higher pH. Clearly further work involving other pH values is necessary in order to be definitive about this point.

In accord with the model of pore development, oxide film weights obtained prior to the appearance of the current minimum in Fig. 1 are representative of the barrier layer which, during the period of rapid current decay prior to the minimum, is growing only very slowly. Weights of films grown for 30 min in both pH 6.1 and 7 electrolytes are approximately equal, 27 μg/cm^2. Using an oxide density of 3.2 g/cm^3 (36, 37) this observation corresponds to an anodizing constant of 16.9 Å/V in contrast to the directly observed value of 12.5 Å/V. Similarly, the steady-state current value of 28.14 μA/cm^2 measured at pH 7 is in contrast to the value of 17 μA/cm^2 obtained in the same environment on electropolished specimens (2). Both of these apparent discrepancies may be attributed to the significant surface roughness derived from the chemical polishing technique. Defining a surface roughness factor as the ratio of the true surface area to the macroscopic surface area, values of 1.35 and 1.65 are derived for the two observations, respectively, in qualitative agreement with SEM observations of the substrate.

Conclusion

The steady-state leakage current observed on anodizing aluminum in a barrier-forming electrolyte, 3 w/o ammonium tartrate, may be regarded as the sum of three components: ionic currents leading to porous oxide formation and to dissolution of aluminum, and an electronic current observed as the difference between the net current and the ionic currents. The net current increases from pH 6.1 to 7, largely due to a doubling in the rate of aluminum dissolution, while the rate of porous oxide formation is relatively pH insensitive. The electronic current decreases with increase in pH, representing 17% of the total current at pH 6.1, but only 1.3% at pH 7. These observations are consistent with an established model of steady state in the barrier oxide layer with an increase in the rate of field-assisted dissolution at the higher pH. The decrease in electronic current with pH is attributed to instability of the oxide surface with a consequent decrease in the residence time of reducible species. A marked nonelectrodic dissolution of aluminum is seen at pH 7, attributed to tartrate ion reduction.

Acknowledgment

This work was sponsored by the National Science Foundation through grants GH 35580 and DMR 72-03201-A01, "Environment-Affected Properties of Oxide Films as Related to Defect Structure."

Manuscript submitted June 1, 1976; revised manuscript received Aug. 2, 1976.

Any discussion of this paper will appear in a Discussion Section to be published in the June 1977 JOURNAL. All discussions for the June 1977 Discussion Section should be submitted by Feb. 1, 1977.

Publication costs of this article were assisted by the University of Connecticut.

REFERENCES

1. P. G. Anderson and O. F. Devereux, *This Journal*, **122**, 267 (1975).
2. Y. H. Choo and O. F. Devereux, *ibid.*, **122**, 1645 (1975).
3. T. A. Libsch and O. F. Devereux, *ibid.*, **122**, 1654 (1975).
4. J. P. O'Sullivan and G. C. Wood, *Proc. R. Soc. London, Ser. A*, **317**, 511 (1970).
5. J. E. Lewis and R. C. Plumb, *This Journal*, **105**, 496 (1958).
6. J. A. Davies, J. P. S. Pringle, R. L. Graham, and F. Brown, *ibid.*, **109**, 999 (1962).
7. J. A. Davies and B. Domeij, *ibid.*, **110**, 849 (1963).
8. J. A. Davies, B. Domeij, J. P. S. Pringle, and F. Brown, *ibid.*, **112**, 675 (1965).
9. T. P. Hoar and N. F. Mott, *J. Phys. Chem. Solids*, **9**, 97 (1959).
10. D. A. Vermilyea, *This Journal*, **110**, 345 (1963).
11. M. A. Heine and M. J. Pryor, *ibid.*, **110**, 1205 (1963).
12. A. J. Brock and G. C. Wood, *Electrochim. Acta*, **12**, 395 (1967).
13. T. P. Hoar, D. C. Mears, and G. P. Rothwell, *Corros. Sci.*, **5**, 279 (1965).
14. G. T. Rogers, P. H. G. Draper, and S. S. Wood, *Electrochim. Acta*, **13**, 251 (1968).
15. L. Young, "Anodic Oxide Films," Academic Press, New York (1961).
16. W. Ch. van Geel, *Physica*, **17**, 761 (1951).
17. W. Ch. van Geel, *Halbleiterprobleme*, **1**, 291 (1955).
18. R. L. Taylor and H. E. Haring, *This Journal*, **103**, 611 (1956).
19. Y. Sasaki, *J. Phys. Chem. Solids*, **13**, 177 (1960).
20. J. F. Dewald, in "Semiconductors," N. B. Hannay, Editor, p. 729, Reinhold, New York (1959).
21. A. K. Vijh, in "Oxides and Oxide Films," J. W. Diggle, Editor, Vol. 2, p. 1, Marcel Dekker, New York (1973).
22. A. C. Smith, *Can. J. Phys.*, **35**, 1151 (1957).
23. A. C. Smith, *ibid.*, **37**, 591 (1959).
24. D. A. Vermilyea, *J. Appl. Phys.*, **27**, 963 (1956).
25. J. W. Diggle, T. C. Downie, and C. W. Goulding, *Chem. Rev.*, **69**, 365 (1969).
26. T. P. Hoar and J. Yahalom, *This Journal*, **110**, 614 (1963).
27. M. S. Hunter and P. F. Towner, *ibid.*, **108**, 139 (1961).
28. J. S. Leach and P. Neufeld, *Corros. Sci.*, **9**, 413 (1969).
29. N. D. Greene, "Experimental Electrode Kinetics," Rensselaer Polytechnic Institute, Troy, N.Y. (1965).
30. ASTM Standard B 137-45, "The Weight of Coating on Anodically Coated Aluminum", *Annual Book of ASTM Standards* Part 6, p. 87, Amer. Soc. for Testing and Materials, Easton, Md. (1972).
31. *Annual Book of ASTM Standards*, Part 23, p. 70, Amer. Soc. for Testing and Materials, Easton, Md. (1972).
32. M. Pourbaix, "Atlas D'Equilibres Electrochimiques, Gauther-Villars & Cie, Paris (1963).
33. D. J. Stirland and R. W. Bicknell, *This Journal*, **106**, 481 (1959).
34. T. A. Libsch and O. F. Devereux, *ibid.*, **123**, 864 (1976).
35. J. S. Enochs and O. F. Devereux, Unpublished.
36. G. Haas, *J. Opt. Soc. Am.*, **39**, 532 (1949).
37. R. C. Plumb, *This Journal*, **105**, 498 (1958).